Supplementary Information for

Theoretical characterizations of the two-photon fluorescent probes for nitric oxide detection: sensing mechanism, photophysical properties and protonation effects

Yawen Jiao,‡[a] Xiaoxu Dong,‡[a] Xin Ran,‡[a] Qiyun Deng,[b] Haibin Xiao,[a] Zhiming Wang*[b] and Tian Zhang*[a]

[a]School of Chemistry and Chemical Engineering, Shandong University of Technology, Zibo 255049, China. E-mail: tzhang@sdut.edu.cn

[b]AIE institute, State Key Laboratory of Luminescent Materials and Devices, Center for Aggregation-Induced Emission, Guangdong Provincial Key Laboratory of Luminescence from Molecular Aggregates, South China University of Technology, Guangzhou 510640, China. E-mail: wangzhiming@scut.edu.cn

† Electronic supplementary information (ESI) available.
‡ These authors contributed equally.

Contents

I. Theoretical formalism for NACME

The non-adiabatic electronic coupling matrix element (NACME), *i.e.*, R_{kl} matrix in eqn (3) was treated as a product of the derivative coupling $R_{kl} = \langle \Phi_f | \hat{P}_{fk} | \Phi_i \rangle \langle \Phi_i | \hat{P}_{fl} | \Phi_f \rangle$, which can be solved via the first-order perturbation theory following Lin *et al*. At the equilibrium position approximately, we get: [S1]

$$\langle \Phi_f | \hat{P}_{fl} | \Phi_i \rangle = -i\hbar \langle \Phi_f | \frac{\partial}{\partial Q_{fl}} | \Phi_i \rangle = -i\hbar \frac{\langle \Phi_f^0 | \partial \hat{U} / \partial Q_{fl} | \Phi_i^0 \rangle}{E_i^0 - E_f^0} \tag{S1}$$

where

$$\langle \Phi_f^0 | \partial \hat{U} / \partial Q_{fl} | \Phi_i^0 \rangle = -\sum_{\sigma} \frac{Z_\sigma e^2}{\sqrt{M_\sigma}} \sum_{\tau=x,y,z} E_{f \leftarrow i,\sigma\tau} L_{\sigma\tau,l} \tag{S2}$$

The transition electric field $E_{f \leftarrow i,\sigma\tau} = \int d\boldsymbol{r} \rho_{fi}^0(\boldsymbol{r}) \frac{e(r_\tau - R_{\sigma\tau})}{|\boldsymbol{r} - \boldsymbol{R}_\sigma|^3}$ can be computed at the TD-DFT level in the Gaussion 16 package, and U is the electron-nuclear potential term in the Hamiltonian.

II. Broadening function for the TPA lineshape

The macroscopic TPA cross section can be obtained from the rotationally averaged TPA strength δ_{tp} in eqn (6) using: [S2]

$$\sigma_{tpa} = \frac{4\pi^3 \alpha a_0^5 \omega^2}{c} \delta_{tp} g(2\omega, \omega_{if}, \Gamma) \tag{S3}$$

The lineshape function $g(2\omega, \omega_{if}, \Gamma)$ describes broadening effects with an empirical damping parameter Γ to describe the spectral broadening of an excitation. Herein, a Lorentzian lineshape function is used for $g(2\omega, \omega_{if}, \Gamma)$.

$$g(2\omega) = \frac{1}{\pi} \frac{\Gamma}{(2\omega - \omega_{if})^2 + \Gamma^2} \tag{S4}$$

where ω is the photon energy, ω_{if} is the excitation energy and Γ is the half width at half maximum (HWHM). The function is normalized to one. By setting $\omega=\omega_{if}/2$, the maximum of the Lorentzian is obtained as,

$$g(\omega_{if}) = \frac{1}{\pi\Gamma} \tag{S5}$$

When this maximum is inserted for $g(2\omega, \omega_{if}, \Gamma)$ in eqn (S3), one obtains eqn (7) in the main text.

III. Energy gap law for non-radiative transitions

In 1950, Huang and Rhys proposed the theory of multiphonon non-radiative transitions, originally developed for the light-emitting from the color center in solids.[S3]

In 1970, Englman and Jortner presented the energy gap law for non-radiative transitions in the strong and weak coupling limits.[S4] In the strong coupling limit, the transition probability is determined by a gaussian function of the energy parameter ($\Delta E - E_M$), where ΔE is the energy gap between the origins of the two electronic states and $2E_M$ is the Stokes shift. The weak coupling limit reveals an exponential (or rather superexponential) dependence of the transition probability on the energy gap ΔE. Indeed, the weak coupling limit prevails for electronic relaxation in large aromatic molecules, while the study of the strong coupling case is of interest for the understanding of unimolecular photochemical reactions which take place in excited electronic states of large molecules.

The non-radiative transition probability is given by:

$$W = \frac{C^2}{\hbar^2} \exp\ (-G) \int_{-\infty}^{\infty} \exp\ \left[-\frac{i\Delta E t}{\hbar} + G_+(t) + G_-(t) \right] dt \qquad \text{(S6)}$$

Note that this result exhibits the dependence of W on the energy gap ΔE.

When the weak coupling limit is encountered, the following result is obtained:

$$W = \frac{C^2 \sqrt{(2\pi)}}{\hbar \sqrt{(\hbar\omega_M \Delta E)}}\ \exp\ \left(-\frac{1}{2} \sum_j \Delta_j^2 \right) \exp\ \left\{ -\frac{\Delta E}{\hbar\omega_M} \left[\log \left(\frac{2\Delta E}{\sum_M \hbar\omega_M \Delta_M^2} \right) - 1 \right] \right\} \qquad \text{(S7)}$$

Let

$$de_M = \frac{1}{2} \sum_{M=1,\ \ldots,\ d} \hbar\omega_M \Delta_M^2 \qquad \text{(S8)}$$

be the contribution of the modes of maximum frequency to E_M, and we assume that there is the same contribution from each of the d normal modes so that $e_M = \frac{1}{2} \hbar\omega_M \Delta_M^2$. Then eqn (S7) can be rewritten in the form:

$$W = \frac{C^2\sqrt{(2\pi)}}{\hbar\sqrt{(\hbar\omega_M \Delta E)}} \ \exp\ \left(-E_M/\hbar\langle\omega\rangle\right) \exp\ \left\{-\frac{\Delta E}{\hbar\omega_M}\ \left[\log\left(\frac{\Delta E}{de_M}\right)-1\right]\right\} \tag{S9}$$

This low temperature result is adequate either for the isolated molecule or for a molecule in an inert medium. eqn (S7) exhibits the energy gap law for the weak coupling limit. As $G \lesssim 1$ we set exp (–G) ~1. Furthermore, as in eqn (S9) $\log\left(\Delta E/de_M\right)$>1,we expect that the parameter:

$$\gamma \equiv \gamma\left(\Delta E,\ e_M,\ d\right) = \log\left(\frac{\Delta E}{de_M}\right)-1 \tag{S10}$$

is positive so that W assumes the form:

$$W = \frac{C^2\sqrt{(2\pi)}}{\hbar\sqrt{(\hbar\omega_M \Delta E)}} \ \exp\ \left(-\gamma\Delta E/\hbar\omega_M\right) \tag{S11}$$

This result exhibits a rough exponential (or rather somewhat stronger than exponential) dependence of the transition probability on the energy gap.

IV. Few-state models for two-photon transition matrix element

Few-states models are obtained by truncating the summations in eqn (5) to include a finite number of excited states.

(I) Assuming k = i, f, $\omega = \omega_{\mathrm{if}}/2$, the two-state model can be written as:

$$S_{(2-\mathrm{state})} = \frac{\langle \mathrm{i}|\hat{\mu}_\alpha|\mathrm{i}\rangle\langle \mathrm{i}|\hat{\mu}_\beta|\mathrm{f}\rangle}{-\omega_{\mathrm{if}}/2} + \frac{\langle \mathrm{i}|\hat{\mu}_\beta|\mathrm{i}\rangle\langle \mathrm{i}|\hat{\mu}_\alpha|\mathrm{f}\rangle}{-\omega_{\mathrm{if}}/2} + \frac{\langle \mathrm{i}|\hat{\mu}_\alpha|\mathrm{f}\rangle\langle \mathrm{f}|\hat{\mu}_\beta|\mathrm{f}\rangle}{\omega_{\mathrm{if}}/2} + \frac{\langle \mathrm{i}|\hat{\mu}_\beta|\mathrm{f}\rangle\langle \mathrm{f}|\hat{\mu}_\alpha|\mathrm{f}\rangle}{\omega_{\mathrm{if}}/2} = \frac{2\mu_{\mathrm{if}}\Delta\mu}{\omega_{\mathrm{if}}/2}$$

So that one obtains eqn (9) in the main text.

(II) Assuming k = i, m, f, $\omega = \omega_{\mathrm{if}}/2$, the three-state model can be expressed as:

$$S_{(3-\mathrm{state})} = S_{(2-\mathrm{state})} + \frac{\langle \mathrm{i}|\hat{\mu}_\alpha|m\rangle\langle m|\hat{\mu}_\beta|\mathrm{f}\rangle + \langle \mathrm{i}|\hat{\mu}_\beta|m\rangle\langle m|\hat{\mu}_\alpha|\mathrm{f}\rangle}{\omega_{im} - \omega_{\mathrm{if}}/2} = \frac{2\mu_{\mathrm{if}}\Delta\mu}{\omega_{\mathrm{if}}/2} + \frac{2\mu_{im}\mu_{m\mathrm{f}}}{\omega_{im} - \omega_{\mathrm{if}}/2}$$

So that one obtains eqn (10) in the main text.

(III) Assuming k = i, m, n, f, $\omega = \omega_{\mathrm{if}}/2$, the four-state model can be formulated as:

$$S_{(4-\mathrm{state})} = S_{(3-\mathrm{state})} + \frac{\langle \mathrm{i}|\hat{\mu}_\alpha|n\rangle\langle n|\hat{\mu}_\beta|\mathrm{f}\rangle + \langle \mathrm{i}|\hat{\mu}_\beta|n\rangle\langle n|\hat{\mu}_\alpha|\mathrm{f}\rangle}{\omega_{in} - \omega_{\mathrm{if}}/2} = \frac{2\mu_{\mathrm{if}}\Delta\mu}{\omega_{\mathrm{if}}/2} + \frac{2\mu_{im}\mu_{m\mathrm{f}}}{\omega_{im} - \omega_{\mathrm{if}}/2} + \frac{2\mu_{in}\mu_{n\mathrm{f}}}{\omega_{in} - \omega_{\mathrm{if}}/2}$$

So that one obtains eqn (11) in the main text.

V. Detailed analyses of TPA properties using the few-state models

(I) In the case of the TPA into a state with a major μ_{if}, the two-state model can be implemented:

For NINO (final state is S_2), μ_{02} = 2.14 a.u., $\Delta\mu = \mu_{22} - \mu_{00}$ = (5.16 – 3.19) a.u. = 1.97 a.u., and ω_{02} = 2.96 eV = 0.11 a.u.

$$S_{(2-\text{state})} = \frac{2\mu_{02}\Delta\mu}{\omega_{02}/2} = \frac{2\times 2.14\times 1.97}{0.11/2} \text{ a.u.} = 153.3 \text{ a.u.}$$

For NINO-TZ (final state is S_1), μ_{01} = 1.73 a.u., $\Delta\mu = \mu_{11} - \mu_{00}$ = (12.10 – 4.81) a.u. = 7.29 a.u., and ω_{01} = 2.94 eV = 0.11 a.u.

$$S_{(2-\text{state})} = \frac{2\mu_{01}\Delta\mu}{\omega_{01}/2} = \frac{2\times 1.73\times 7.29}{0.11/2} \text{ a.u.} = 458.6 \text{ a.u.}$$

For PYSNO (final state is S_1), μ_{01} = 2.65 a.u., $\Delta\mu = \mu_{11} - \mu_{00}$ = (10.75 – 1.77) a.u. = 8.98 a.u., ω_{01} = 2.42 eV = 0.09 a.u.

$$S_{(2-\text{state})} = \frac{2\mu_{01}\Delta\mu}{\omega_{01}/2} = \frac{2\times 2.65\times 8.98}{0.09/2} \text{ a.u.} = 1057.6 \text{ a.u.}$$

(II) In the case of the TPA into the S_2 state with a minor μ_{if}, the three-state model can be implemented:

For PYSNO, μ_{02} = 1.36 a.u., $\Delta\mu = \mu_{22} - \mu_{00}$ = (6.94 – 1.77) a.u. = 5.17 a.u., and ω_{02} = 3.13 eV = 0.12 a.u.; μ_{01} = 2.65 a.u., μ_{12} = 5.31 a.u., and $\omega_{01} - \omega_{02}/2$ = (2.42 – 3.13/2) eV = 0.86 eV = 0.03 a.u.

$$S_{(3-\text{state})} = \frac{2\mu_{02}\Delta\mu}{\omega_{02}/2} + \frac{2\mu_{01}\mu_{12}}{\omega_{01}-\omega_{02}/2} = \left(\frac{2\times 1.36\times 5.17}{0.12/2} + \frac{2\times 2.65\times 5.31}{0.03}\right) \text{ a.u.} = (234.4 + 938.1) \text{ a.u} = 1172.5 \text{ a.u.}$$

For PYSNO-TZ, μ_{02} = 0.53 a.u., $\Delta\mu = \mu_{22} - \mu_{00}$ = (5.98 – 2.36) a.u. = 3.62 a.u., and ω_{02} = 3.42 eV = 0.13 a.u.; μ_{01} = 2.87 a.u., μ_{12} = 6.18 a.u., and $\omega_{01} - \omega_{02}/2$ = (2.80 – 3.42/2) eV = 1.09 eV = 0.04 a.u.

$$S_{(3-\text{state})} = \frac{2\mu_{02}\Delta\mu}{\omega_{02}/2} + \frac{2\mu_{01}\mu_{12}}{\omega_{01}-\omega_{02}/2} = \left(\frac{2\times 0.53\times 3.62}{0.13/2} + \frac{2\times 2.87\times 6.18}{0.04}\right) \text{ a.u.} = (59.0 + 886.8) \text{ a.u} = 945.8 \text{ a.u.}$$

(III) In the case of the TPA into the S_3 state with a minor μ_{if}, the four-state model can be implemented:

For PYSNO, μ_{03} = 0.48 a.u., $\Delta\mu = \mu_{33} - \mu_{00}$ = (6.37 – 1.77) a.u. = 4.60 a.u., and ω_{03} = 3.47 eV = 0.13 a.u.; μ_{01} = 2.65 a.u., μ_{13} = 1.56 a.u., and $\omega_{01} - \omega_{03}/2$ = (2.42 – 3.47/2) eV = 0.69 eV = 0.03 a.u.; μ_{02} = 1.36 a.u., μ_{23} = 7.42 a.u., and $\omega_{02} - \omega_{03}/2$ = (3.13 – 3.47/2) eV = 1.40 eV = 0.05 a.u.

$$S_{(4-\text{state})} = \frac{2\mu_{03}\Delta\mu}{\omega_{03}/2} + \frac{2\mu_{01}\mu_{13}}{\omega_{01}-\omega_{03}/2} + \frac{2\mu_{02}\mu_{23}}{\omega_{02}-\omega_{03}/2} = \left(\frac{2\times0.48\times4.60}{0.13/2} + \frac{2\times2.65\times1.56}{0.03} + \frac{2\times1.36\times7.42}{0.05}\right) \text{a.u.}$$

$$= (67.9 + 275.6 + 403.6)\ \text{a.u} = 747.1\ \text{a.u.}$$

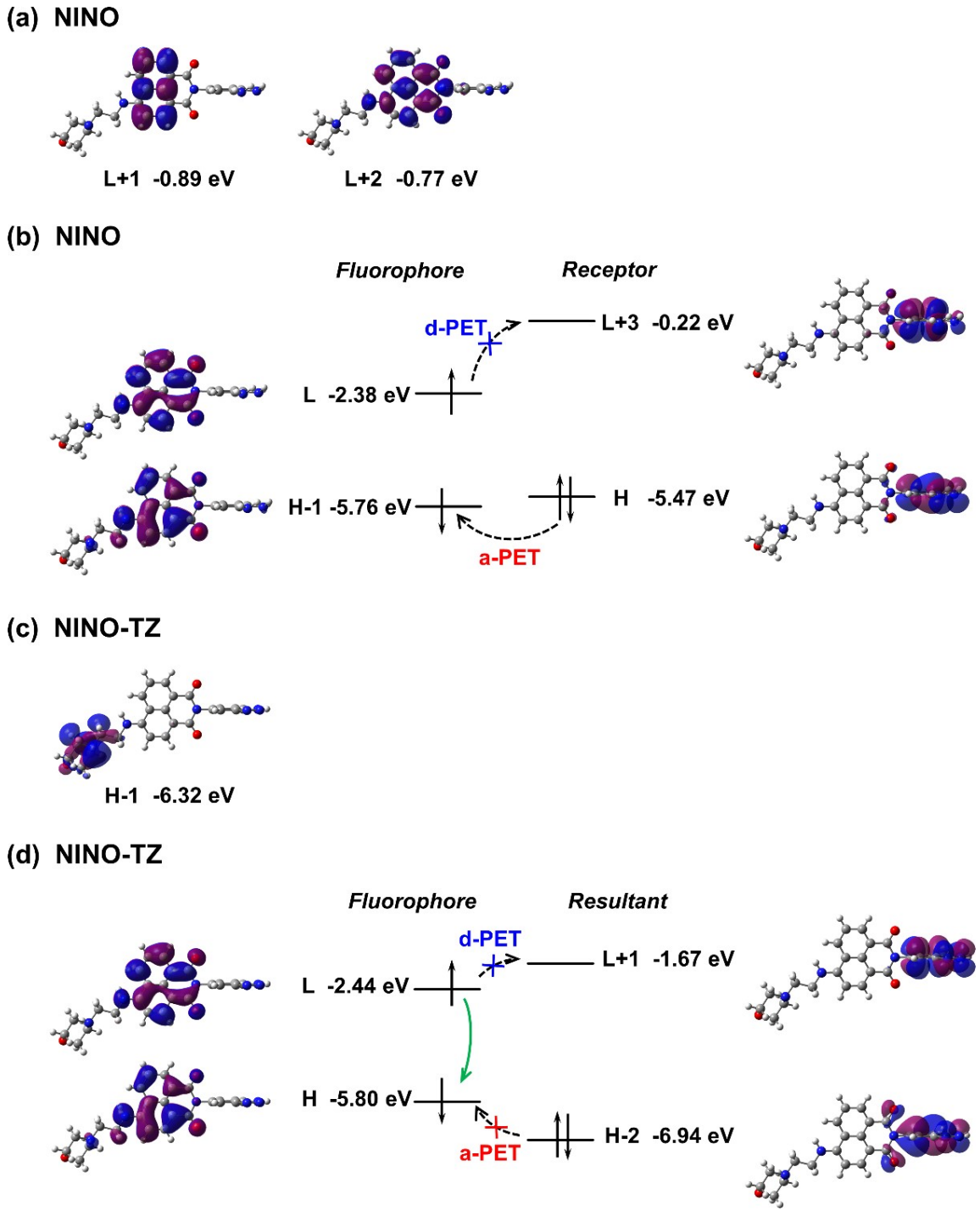

Fig. S1 Eliminated orbitals during the mapping process (a, c) and orbital diagrams to display the "on/off" PET (b, d) for NINO and NINO-TZ.

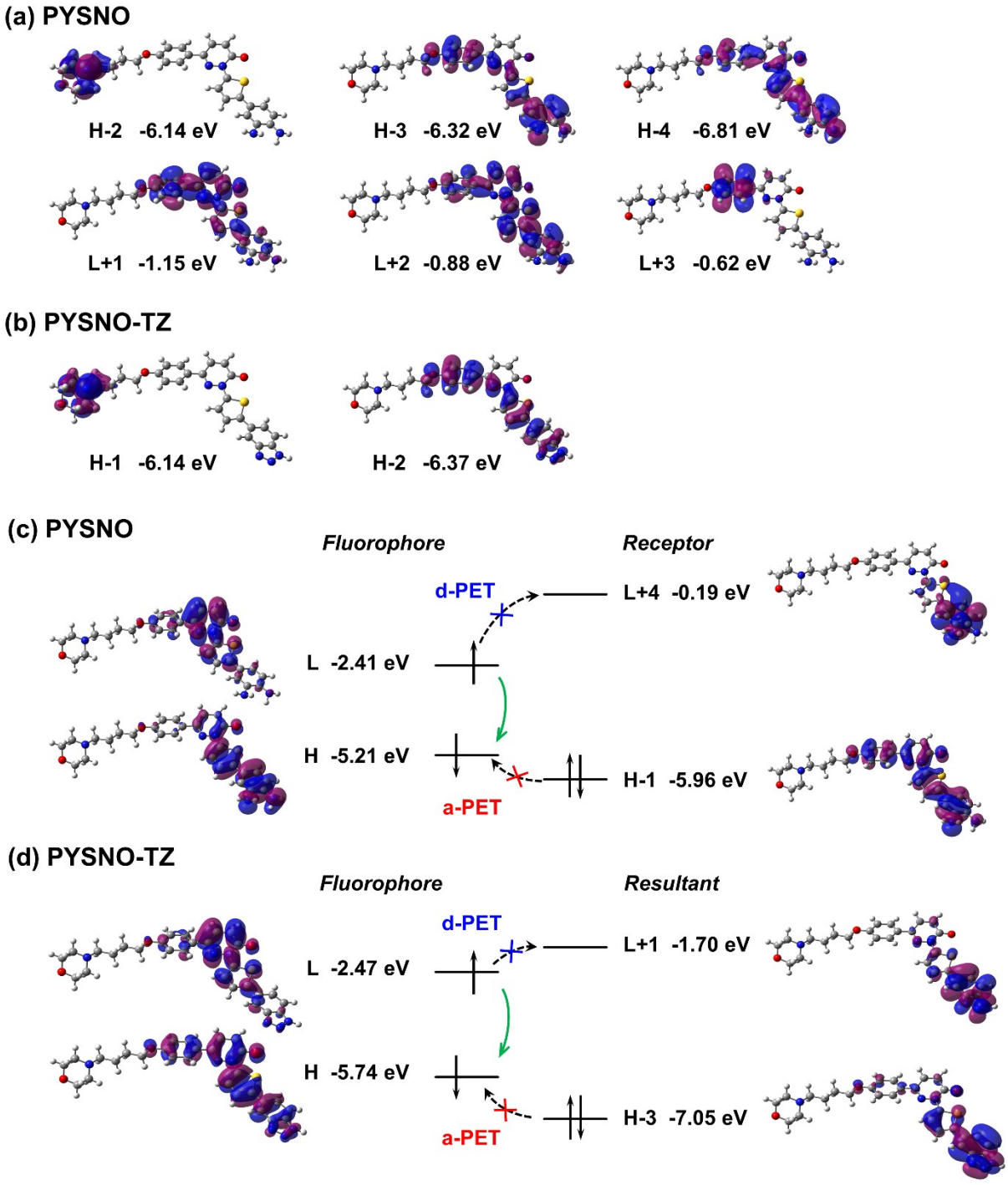

Fig. S2 Eliminated orbitals during the mapping process (a, b) and orbital diagrams to display the "on/off" PET (c, d) for PYSNO and PYSNO-TZ.

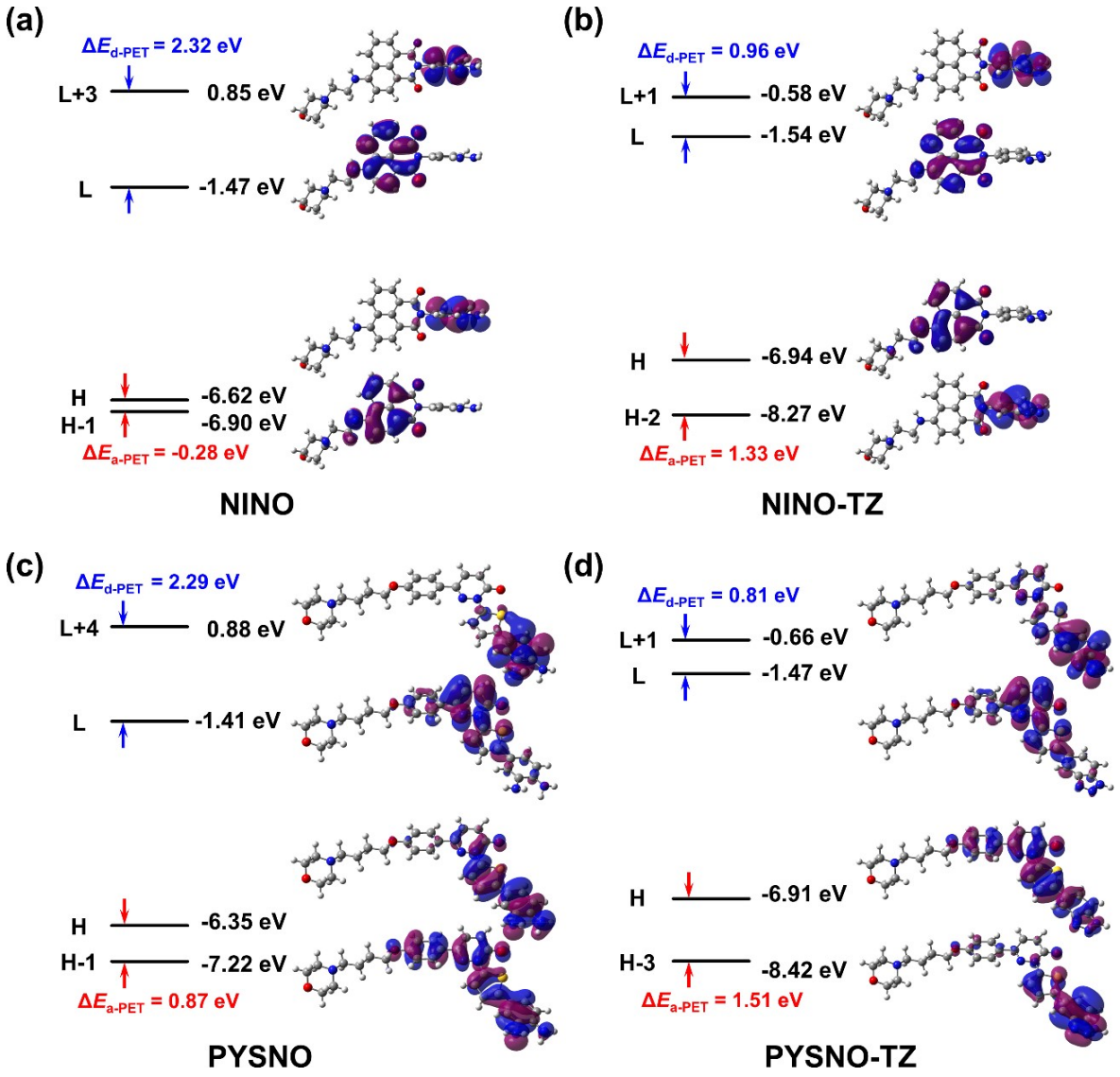

Fig. S3 Four-level FMO diagrams with the spatial distributions for NINO (a), NINO-TZ (b), PYSNO (c) and PYSNO-TZ (d) at the M062X/def2SVP level.

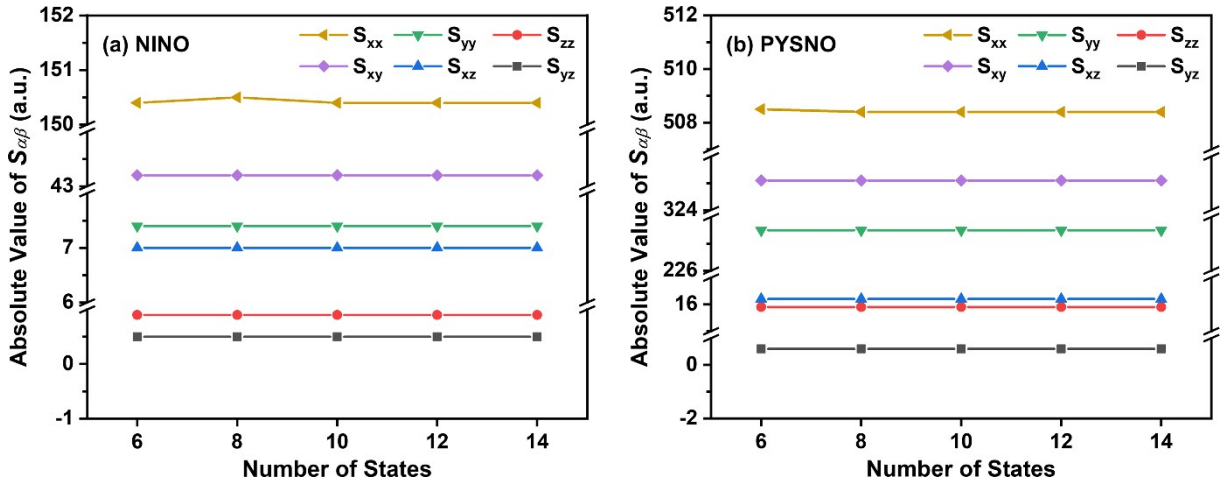

Fig. S4 Absolute value of $S_{\alpha\beta}$ (a.u.) versus number of states for the representative S_2 states of NINO (a) and PYSNO (b) in water.

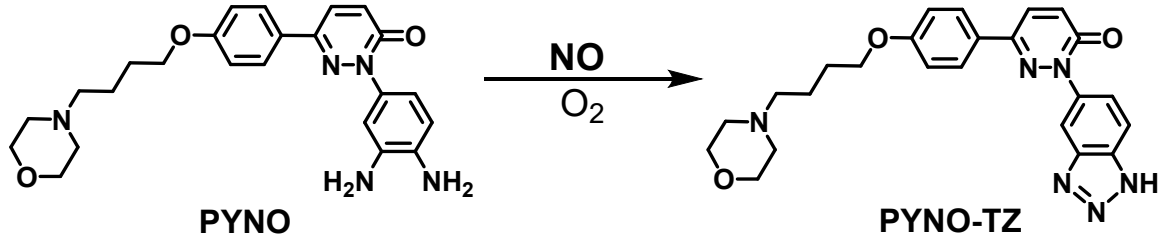

Fig. S5 PYNO and its NO-adduct PYNO-TZ under aerobic condition.

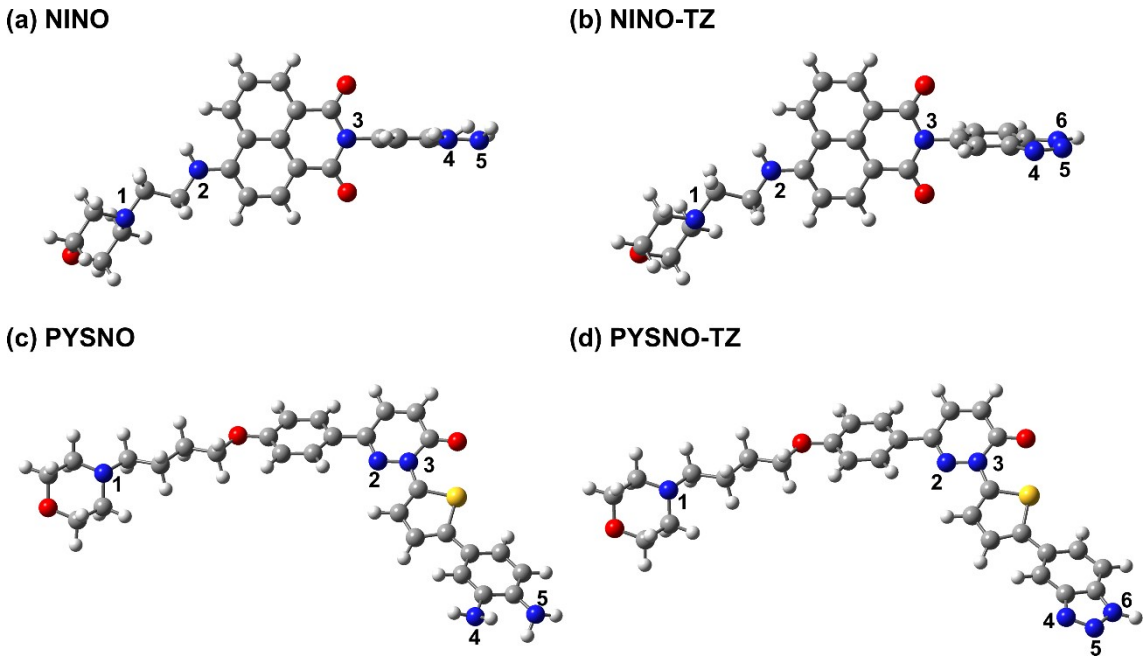

Fig. S6 Assigned numbers for five N atoms in the probes and six N atoms in the reaction products for NINO (a), NINO-TZ (b), PYSNO (c) and PYSNO-TZ (d).

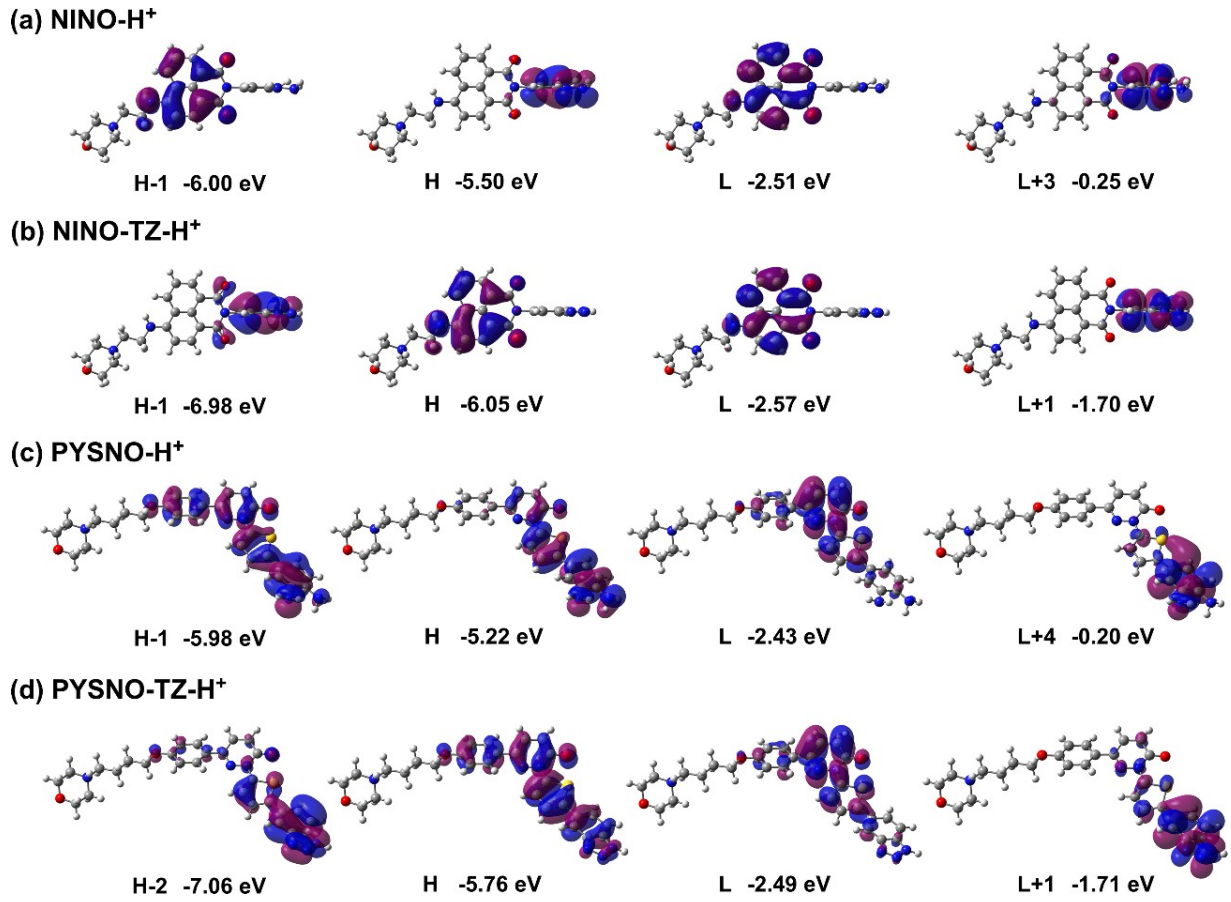

Fig. S7 Spatial distributions involved in the four-level FMO diagrams for NINO-H$^+$ (a), NINO-TZ-H$^+$ (b), PYSNO-H$^+$ (c), and PYSNO-TZ-H$^+$ (d).

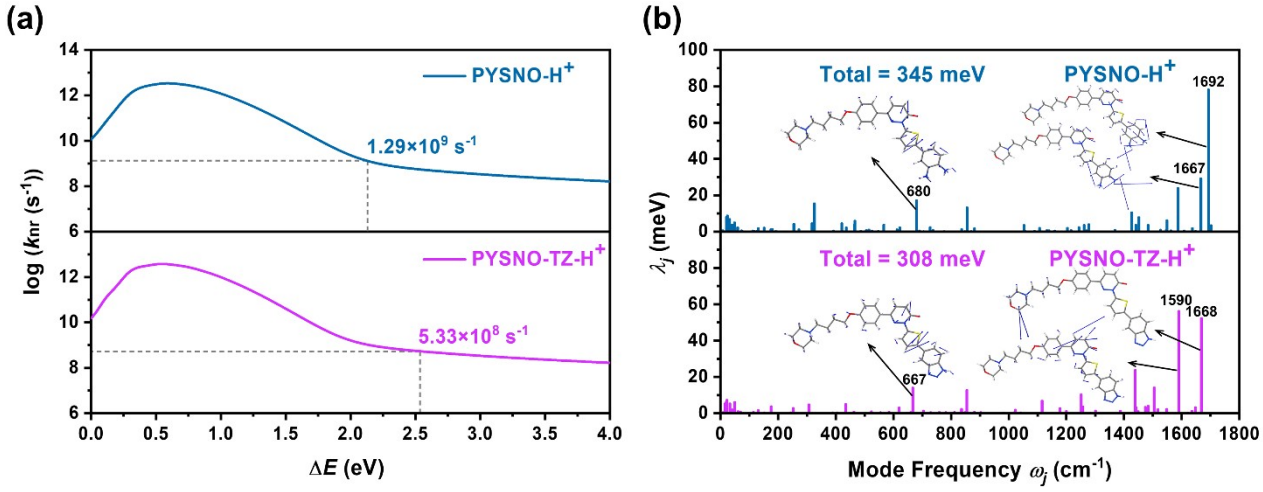

Fig. S8 Calculated logarithm of the non-radiative decay rate log (k_{nr}) *versus* the energy gap ΔE (T = 298 K). The vertical dash line indicates the position of the adiabatic energy gap ΔE_{ad} (a) and relaxation energies λ_j (b) *versus* mode frequency ω_j for PYSNO-H$^+$ and PYSNO-TZ-H$^+$.

Table S1 Calculated absorption and emission wavelengths (in nm) by using different functionals based on the $S_0(S_1)$-optimized geometries at the level of B3LYP/6-31+G(d). The 6-311G(d,p) basis set and different solvent models (LR-PCM and SS-PCM) were further applied to the chosen B3LYP functional. The experimental peak values (Exp.) in water are also given.

Abs.								
Functional	B3LYP		B3LYP	PBE33	BMK	M062X	CAM-B3LYP	
Basis Set	6-311G(d,p)		6-31+G(d)					
PCM	LR-PCM	SS-PCM	LR-PCM					Exp.
NINO	420	440	427	384	356	320	312	430
NINO-TZ	421	441	429	396	388	382	381	430
PYSNO	512	662	509	439	414	391	390	460
PYSNO-TZ	443	447	445	402	386	372	373	402
Emi.								
NINO-TZ	477	588	502	444	433	426	423	530
PYSNO	670	1012	708	572	534	497	492	581
PYSNO-TZ	548	601	584	502	480	463	464	548

Table S2 The excitation energies E_{opa} (eV), OPA wavelengths λ_{opa} (nm), oscillator strengths f and the transition natures of the lowest three excited states for NINO, NINO-TZ, PYSNO and PYSNO-TZ in water. Experimental values are also presented in parentheses.

	State	E_{opa}	λ_{opa}	f	Transition nature
NINO	S_1	2.62	473	0.00	H→L 99.6%
	S_2	2.96	420 (430)	0.33	H-1→L 97.0%
	S_3	3.11	399	0.00	H-2→L 76.6%
NINO-TZ	S_1	2.94	421 (430)	0.33	H→L 97.0%
	S_2	3.05	407	0.00	H-1→L 99.7%
	S_3	3.71	334	0.00	H→L+1 99.6%
PYSNO	S_1	2.42	512 (460)	0.41	H→L 99.1%
	S_2	3.13	397 (402)	0.14	H-1→L 97.6%
	S_3	3.47	358	0.02	H-3→L 94.3%
PYSNO-TZ	S_1	2.80	443 (402)	0.56	H→L 99.1%
	S_2	3.42	363	0.02	H-2→L 94.3%
	S_3	3.45	360	0.00	H-1→L 99.9%

Table S3 The electronic energies $E_{S_1(S_2)}$ (a.u.) at the $S_1(S_2)$ minimum, the energy differences ΔE (eV) and internal conversion rate constants k_{ic} (s^{-1}) from S_2 to S_1 state for NINO, NINO-TZ, PYSNO and PYSNO-TZ in water.

	E_{S_1}	E_{S_2}	ΔE	k_{ic}
NINO	-1429.3843	-1429.3548	0.80	5.12×10^{10}
NINO-TZ	-1482.2682	-1482.2422	0.71	7.16×10^{10}
PYSNO	-1983.5920	-1983.5661	0.71	7.16×10^{10}
PYSNO-TZ	-2036.4862	-2036.4630	0.63	9.63×10^{10}

Table S4 The oscillator strengths *f*, vertical emission energies E_{emi} (eV) and radiative decay rate constants k_r (s^{-1}) from S_1 to S_0 state for NINO, NINO-TZ, PYSNO and PYSNO-TZ in water.

	f	E_{emi}	k_r
NINO	0.0007	1.49	6.74×10^{4}
NINO-TZ	0.25	2.60	7.33×10^{7}
PYSNO	0.48	1.85	7.12×10^{7}
PYSNO-TZ	0.66	2.26	1.46×10^{8}

Table S5 The excitation energies E_{tpa} (eV), TPA wavelengths λ_{tpa} (nm), TPA strength δ_{tp} (a.u.) and cross sections σ_{tpa} (GM) of the lowest ten excited states for NINO, NINO-TZ, PYSNO and PYSNO-TZ in water.

	E_{tpa}	λ_{tpa}	δ_{tp}	σ_{tpa}		E_{tpa}	λ_{tpa}	δ_{tp}	σ_{tpa}
NINO	2.53	978	273	1	NINO-TZ	2.88	859	5630	34
	2.90	853	4880	30		3.04	814	1570	11
	3.10	798	1930	14		3.74	661	1000	10
	3.44	719	582	5		3.80	651	58	1
	3.86	641	6	0		4.00	618	13	0
	4.02	615	205	2		4.02	615	176	2
	4.07	608	61	1		4.07	608	459	6
	4.08	606	4	0		4.33	571	2660	37
	4.33	571	1280	18		4.37	566	1310	18
	4.36	567	18	0		4.41	561	4260	61
PYSNO	2.35	1052	189000	765	PYSNO-TZ	2.71	913	29200	157
	3.09	800	106000	742		3.40	727	137000	1161
	3.45	717	72900	636		3.46	715	74	1
	3.51	705	55	0		3.54	699	47000	432
	3.63	681	70600	682		3.93	629	1450	16
	3.84	644	72900	788		4.04	612	26900	322
	3.92	631	9230	104		4.11	602	48800	604
	3.96	625	54200	623		4.20	589	4070	53
	4.14	597	5	0		4.25	582	18300	242
	4.23	585	7840	103		4.26	581	12600	168

Table S6 Two-photon transition matrix element $S_{\alpha\beta}$ (a.u.) for the representative S_2 states of NINO and PYSNO in water.

	Number of states	S_{xx}	S_{yy}	S_{zz}	S_{xy}	S_{xz}	S_{yz}
NINO	6	150.40	-7.40	-0.90	-43.20	-7.00	-0.50
	8	150.50	-7.40	-0.90	-43.20	-7.00	-0.50
	10	-150.40	7.40	0.90	43.20	7.00	0.50
	12	150.40	-7.40	-0.90	-43.20	-7.00	-0.50
	14	150.40	-7.40	-0.90	-43.20	-7.00	-0.50
PYSNO	6	508.50	227.50	-0.60	-325.10	16.20	-15.90
	8	-508.40	-227.50	0.60	325.10	-16.20	15.90
	10	508.40	227.50	-0.60	325.10	16.20	-15.90
	12	-508.40	-227.50	0.60	325.10	-16.20	15.90
	14	508.40	227.50	-0.60	-325.10	16.20	-15.90

Table S7 The excitation energies E_{tpa} (eV), TPA wavelengths λ_{tpa} (nm), TPA strength δ_{tp} (a.u.) and cross sections σ_{tpa} (GM) of the lowest ten excited states for PYNO and PYNO-TZ in water.

	E_{tpa}	λ_{tpa}	δ_{tp}	σ_{tpa}		E_{tpa}	λ_{tpa}	δ_{tp}	σ_{tpa}
PYNO	2.94	841	236	1	PYNO-TZ	3.35	738	2810	23
	3.46	715	3180	28		3.75	659	14	0
	3.86	641	1240	14		3.83	646	1340	14
	3.87	639	23	0		3.94	628	2990	34
	4.04	612	425	5		4.19	590	14600	188
	4.08	606	247	3		4.24	583	0	0
	4.41	561	9730	139		4.37	566	2700	38
	4.44	557	1710	25		4.41	561	942	13
	4.54	545	791	12		4.47	553	805	12
	4.55	544	220	3		4.64	533	591	9

Table S8 The electronic energies (a.u.) and relative values (eV) of the optimized geometries for the protonated conformations named NINO-H^+, NINO-TZ-H^+, PYSNO-H^+ and PYSNO-TZ-H^+. The site numbers can be referred to Fig. S6.

	Site	Energy	Relative		Site	Energy	Relative
NINO-H^+	1	-1429.5983	0.00	PYSNO-H^+	1	-1983.7557	0.00
	2	-1429.5692	0.74		2	-1983.7215	0.93
	3	-1429.5335	1.71		3	-1983.6702	2.33
	4	-1429.5859	0.28		4	-1983.7368	0.51
	5	-1429.5859	0.28		5	-1983.7369	0.51
NINO-TZ-H^+	1	-1482.5093	0.00	PYSNO-TZ-H^+	1	-2036.6658	0.00
	2	-1482.4813	0.76		2	-2036.6300	0.97
	3	-1482.4427	1.81		3	-2036.5783	2.38
	4	-1482.4915	0.48		4	-2036.6442	0.59
	5	-1482.4744	0.95		5	-2036.6263	1.07
	6	-1482.4460	1.72		6	-2036.5986	1.83

Table S9 The excitation energies E_{opa} (eV), corresponding OPA wavelengths λ_{opa} (nm), oscillator strengths f and transition natures of the lowest three excited states for NINO-H^+, NINO-TZ-H^+, PYSNO-H^+ and PYSNO-TZ-H^+ in water.

	State	E_{opa}	λ_{opa}	f	Transition nature
NINO-H^+	S_1	2.51	493	0.00	H→L 99.6%
	S_2	3.08	403	0.34	H-1→L 97.0%
	S_3	3.43	361	0.00	H-2→L 98.5%
NINO-TZ-H^+	S_1	3.06	405	0.35	H→L 97.0%
	S_2	3.79	327	0.00	H-1→L 65.9%
	S_3	3.92	316	0.00	H→L+1 99.7%
PYSNO-H^+	S_1	2.41	513	0.41	H→L 99.1%
	S_2	3.13	396	0.14	H-1→L 97.7%
	S_3	3.48	356	0.02	H-2→L 93.9%
PYSNO-TZ-H^+	S_1	2.80	443	0.56	H→L 99.1%
	S_2	3.44	360	0.02	H-1→L 93.2%
	S_3	3.59	345	0.00	H→L+1 91.2%

Table S10 The oscillator strengths *f*, vertical emission energies E_{emi} (eV) and radiative decay rate constants k_r (s^{-1}) from S_1 to S_0 state for NINO-H^+, NINO-TZ-H^+, PYSNO-H^+ and PYSNO-TZ-H^+ in water.

	f	E_{emi}	k_r
NINO-H^+	0.0006	1.40	5.10×10^4
NINO-TZ-H^+	0.27	2.69	8.47×10^7
PYSNO-H^+	0.48	1.85	7.12×10^7
PYSNO-TZ-H^+	0.66	2.26	1.46×10^8

Table S11 The excitation energies E_{tpa} (eV), TPA wavelengths λ_{tpa} (nm), TPA strength δ_{tp} (a.u.) and cross sections σ_{tpa} (GM) of the lowest ten excited states for NINO-H^+, NINO-TZ-H^+, PYSNO-H^+ and PYSNO-TZ-H^+ in water.

	E_{tpa}	λ_{tpa}	δ_{tp}	σ_{tpa}		E_{tpa}	λ_{tpa}	δ_{tp}	σ_{tpa}
NINO-H^+	2.37	1044	425	2	NINO-TZ-H^+	3.05	811	2890	20
	3.07	806	2580	18		3.71	667	81	1
	3.30	749	753	6		3.94	628	409	5
	3.79	653	3	0		4.04	612	106	1
	3.92	631	63	1		4.05	611	777	9
	3.95	626	25	0		4.23	585	413	5
	4.05	611	127	2		4.36	567	6	0
	4.30	575	3	0		4.42	560	695	10
	4.37	566	444	6		4.48	552	6570	97
	4.49	551	5760	85		4.65	532	1710	27
PYSNO-H^+	2.35	1052	193000	781	PYSNO-TZ-H^+	2.71	913	30900	166
	3.09	800	101000	707		3.42	723	140000	1200
	3.47	713	83300	735		3.55	697	44100	407
	3.62	683	67400	647		3.93	629	1590	18
	3.83	646	70500	758		4.03	614	26300	313
	3.92	631	9870	111		4.11	602	45500	563
	3.96	625	55300	636		4.20	589	4850	63
	4.13	599	19	0		4.26	581	31900	424
	4.22	586	9730	127		4.27	579	519	7
	4.28	578	33000	443		4.34	570	4140	57

References

S1 S. H. Lin, *J. Chem. Phys.*, 1966, **44**, 3759-3767.
S2 W. L. Peticolas, *Annu. Rev. Phys. Chem.*, 1967, **18**, 233-260.
S3 K. Huang and A. Rhys, *Proc. R. Soc. Lond. A*, 1950, **204**, 406-423.
S4 R. Englman and J. Jortner, *Mol. Phys.*, 1970, **18**, 145-164.